AIAA JOURNAL
Vol. 34, No. 5, May 1996

Experimental Study of a Normal Shock/Homogeneous Turbulence Interaction

S. Barre,* D. Alem,† and J. P. Bonnet‡
Université de Poitiers, F-86036 Poitiers Cedex, France

A new method is used to generate a quasihomogeneous isotropic turbulent supersonic flow at Mach number 3. The interaction with a normal shock wave is analyzed by means of hot-wire anemometry and laser Doppler velocimetry. Preliminary results show that the usual behavior of unperturbed turbulence is observed (isotropy, spectra, integral scales, and decay). The shock wave increases the longitudinal fluctuating velocities in agreement with Ribner's theory. Increase of the high-frequency components and decrease of the integral longitudinal scales are observed at the traverse of the shock.

I. Introduction

THE presence of shock waves is an important feature that can play a crucial role in supersonic flows. It appears immediately to those who want to study compressible flows and mainly compressible turbulence that a key point for the understanding and modeling of such flows is to know what happens when a turbulent flow interacts with a shock wave.

This event occurs in many applications of practical interest such as, for example, the shock-wave/boundary-layer interaction. This configuration was extensively studied for many years by experimental as well as numerical methods. Some review articles[1–3] summarize the main results concerning this particular configuration. However, when predictions are concerned, specific models have to be built to properly take into account the drastic modification of the turbulent field subjected to strong pressure gradients.

Unfortunately this very complex configuration, where streamline curvature and unsteady separation problems both occur, makes the study and the prediction of the pure shock wave/turbulence interaction difficult. This is why a new kind of investigation has to be done by studying a simpler case. Such a basic configuration is the interaction between a normal shock and a homogeneous and isotropic turbulent field. The main advantage of such an effort is to isolate the net effect of the strong gradients of mean quantities imposed by the shock wave. This basic configuration has many advantages for both experiments and computations. For the experiments, it reduces the number of geometrical parameters, whereas for numerical predictions, analytical theories as well as advanced [large eddy simulation, direct Navier–Stokes simulation (DNS), eddy-damped quasinormal Markovianized] methods can be applied and compared. This effect on a decaying turbulence can be studied experimentally to deduce the fundamental behavior of such interaction and help modeling compressible turbulent flows including steady or unsteady shock waves.

Early theoretical work concerning this problem was done in the 1950s.[4–10] All of them are based on the linear analysis of a plane disturbance interacting with a shock wave. Ribner,[4–6] in particular, investigated how a shock wave is perturbed by an impinging single shear wave. The theory, later on called Ribner's theory, is, in fact, mostly based on the mode theory developed by Kovasznay[11] and extended to the shock problem by focusing mainly on the acoustic field generated by the interaction with the shock wave.

More recently, numerical simulations of such flows emerge. The calculations of both Rotman[12] and Lee et al.[13,14] show, among other results, that the vorticity amplification predicted are in good agreement with linear theories. As can be expected from linear analysis, DNS studies of Lee et al.[13,14] and Hannapel and Friedrich[15] show how isotropic turbulence becomes axisymmetric after the shock. The evolution of turbulent spectra across the shock exhibits a bigger amplification of the large wave numbers compared with lower ones. Consequently the longitudinal integral length scales are decreased, whereas the lateral one seems unaffected by the shock interaction.

Most of the previous experimental work done in this area is devoted to shock-wave/boundary-layer or free shear layer interactions. In this configuration an oblique shock wave interacts with the boundary layer or the mixing layer. It has been shown that, in these conditions, if the shock is strong enough, the flow separates near the interaction (in the boundary-layer case) and becomes unsteady because of shock oscillations.[16,17] Concerning the evolution of turbulent quantities across the interaction it has been shown, for example, that the turbulence intensities and the anisotropy ratio are increased through the interaction.[16,18] The same kind of results are available for oblique shock wave/shear layers interactions. Data show a high amplification of the turbulence intensities that depends on the shock strength.[19–23]

Another kind of research was performed in a shock tube to study the pure interaction between a normal traveling shock wave reflected on the end wall of a shock tube and then interacting with the flow induced by the incident shock[24,25] or by the wake of a perfored plate.[26,27] All of these experiments show a strong increase of density fluctuations through the shock, but there are few data on the behavior of the velocity field.

It is clear, at this stage, that more fundamental experimental work is needed to clarify the basic mechanism of the shock/turbulence interaction. As previously mentioned, a convenient configuration can be the interaction of a homogeneous and isotropic turbulence with a normal shock. Only a few attempts have been made to study such a flow because of the limited number of possible experimental configurations. Blin[28] and Jacquin et al.[23] create a supersonic quasihomogeneous turbulent flow using a grid as a sonic throat. The flow downstream of the grid is supersonic with a relatively low Mach number (1.7) but with parasitic shock waves. These authors have demonstrated that the turbulence obtained after a grid generating a supersonic flow does not have all of the properties needed for the accurate study of the turbulence. They have analyzed the flow by means of laser Doppler velocimetry. The obtained supersonic flow is shocked by means of a second throat creating a pure normal shock wave/free turbulence interaction. Unfortunately, experimental difficulties due to the very low turbulence level (close to the noise level of the anemometer) leads to a great difficulty in interpreting the results. On other hand, Debiève and Lacharme[29] obtain a quasihomogeneous turbulence by generating perturbations in the settling chamber of a supersonic wind tunnel at Mach 2.3. They show that, after the expansion in the nozzle, the turbulent

Received Nov. 18, 1994; presented as Paper 95-0579 at the AIAA 33rd Aerospace Sciences Meeting, Reno, NV, Jan. 9–12, 1995; revision received Dec. 4, 1995; accepted for publication Jan. 27, 1996.

*Research Scientist, Laboratoire d'Etudes Aerodynamiques, Centre d'Etudes Aerodynamiques et Thermiques. Member AIAA.

†Graduate Student, Laboratoire d'Etudes Aerodynamiques, Centre d'Etudes Aerodynamiques et Thermiques.

‡Research Director, Laboratoire d'Etudes Aerodynamiques, Centre d'Etudes Aerodynamiques et Thermiques. Member AIAA.

field becomes strongly nonisotropic and that the turbulence level is drastically decreased leading to experimental difficulties.

To avoid the problems encountered by the aforementioned authors, we will use, in the present work, a different configuration to obtain a homogeneous and isotropic turbulent field at a Mach 3 supersonic speed. This will be obtained by use of a new concept hereafter denoted multinozzle. This flow will interact with a normal shock wave generated by a Mach effect in the center of the test section.

After a brief description of this experimental setup we will give some new experimental results concerning the evolution of turbulent intensities, spectra, and lengths scales. All of these results will be discussed in the last part of this paper.

II. Experimental Facility and Apparatus

A. Wind Tunnel

The experiments are conducted in a square section, supersonic wind tunnel (150×150 mm^2) driven by a hypersonic ejector ($M = 6$). The temperature is stabilized by a bed of small nickel balls located in the plenum chamber. The adiabatic condition for the walls is approximately achieved through a slight preheating of the nickel balls before the run ($Tt \approx 300$ K), ensuring a recovery temperature very close to the room temperature. The typical run time is about 30–40 s. The stagnation pressure is $0.9\ 10^5$ Pa, and the resulting unit Reynolds number is about 10^7/m.

B. Multinozzle and Shock Generation System

The homogeneous and isotropic turbulent field that may interact with the normal shock wave is obtained by placing a multinozzle in the wind tunnel. The principle of nozzle is to create a kind of turbulence grid by the use of a large number of small nozzles to produce the supersonic flow. In this experiment a 150×150-mm^2 multinozzle made of $625(25 \times 25)$ small Mach 3 individual axisymmetric nozzles is placed in the wind tunnel. Each nozzle generates a Mach 3 flow. The exit section of each nozzle is a 6×6-mm^2 square that gives an equivalent mesh size of 6 mm. It can be expected that the confluence of the flows creates an homogeneous and isotropic turbulent field.

The shock generator is made of two wedges creating a Mach effect in the center of the test section. A schematic view of the entire experimental configuration is given in Fig. 1. The shock/turbulence interaction is investigated along the wind-tunnel axis where the Mach effect can be considered as a pure normal shock wave. The reference axis is given in Fig. 1.

C. Hot-Wire Anemometer and Laser Doppler Velocimeter

Most of the investigations presented in this paper were performed using constant temperature anemometry. The anemometer is a DANTEC 55M10 that is equipped with a symmetrical 55M12 bridge that had been shown to be more stable at high frequency than the standard bridge.[30] The probes are DANTEC 55P11 model with a reduced gap of about 0.7–0.8 mm between the prongs and a 2.5-μm platinum-plated tungsten wire. The wires are slightly slacked to avoid parasitic strain gauge effects. The aspect ratio is about 300, more than convenient for these measurements. Typical bandwidths are greater than 300 kHz. The laser Doppler velocimeter is a two-dimensional one. It uses forward reception process. The fringe spacing is 12 μm. The flow is seeded in the settling chamber by SiO_2 particles (typical size less than 1 μm). The data are processed by an Aerometrics DSA system.

III. Preliminary Results

A. Qualification of the Incoming Turbulence

Figure 2 shows a long-exposure-time (1 ms) schlieren visualization of the flow immediately after the multinozzle. A Mach wave system issued from the trailing edges of the small nozzles can be observed. It can be noticed that all of these waves cannot be detected on shadowgraph visualizations of this flow obtained by focusing the light 3 m after the wind-tunnel axis. So, considering the good sensitivity of this visualization system, it is possible to assume that these shocks are weak. Figure 3 shows another schlieren photograph taken at a downstream distance of $X = 800$ mm ($\approx$130 mesh size). At this location, the Mach waves are practically nonobservable, and so it is possible to consider that after a certain number of mesh size

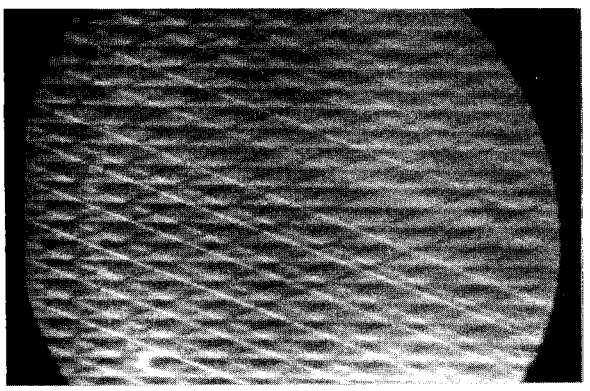

Fig. 2 Schlieren photograph (1-ms exposure time) of the flow just downstream of the multinozzle (flow is from left to right).

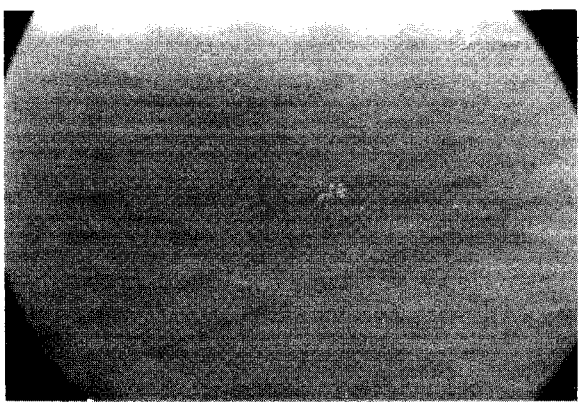

Fig. 3 Schlieren photograph (1-ms exposure time) taken at $X = 800$ mm downstream of the multinozzle (flow is from left to right).

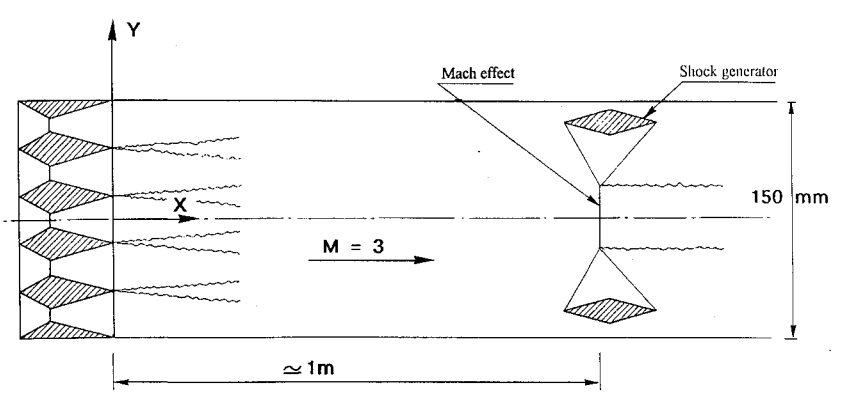

Fig. 1 Sketch of the experimental setup.

downstream of the multinozzle all of this wave system is sufficiently damped. It can then be argued that the effect of this wave system on the homogeneity of the flow is negligible. Furthermore, it has been confirmed both by pitot and hot-wire measurements that the mean and turbulent fields are homogeneous in all of the test sections except those close to the wind tunnel walls and in the near wake of the multinozzle. It has also been verified by means of two-dimensional laser Doppler anemometry that the turbulent field is almost isotropic at least in the X–Y plane. That is, $\langle u' \rangle \approx \langle v' \rangle$ and $\overline{u'v'} \approx 0$, where $\langle u' \rangle$ and $\langle v' \rangle$ are, respectively, the rms values of the longitudinal (X axis) and lateral (Y axis) velocity fluctuations. Figure 4 shows the evolution of the anisotropy ratio along the wind-tunnel axis. Within the experimental uncertainties, the longitudinal and lateral velocity fluctuations are of the same order. Figure 5 shows the longitudinal to lateral velocity fluctuations correlation coefficient along the wind-tunnel axis. It appears that this coefficient is close to zero for the present turbulent field.

At this stage it is possible to assume that, sufficiently downstream of the multinozzle (after about 10 times the mesh size) and in the center part of the working section, a homogeneous mean flow is obtained that convects a decaying homogeneous and isotropic turbulent field. It has been verified by hot-wire measurements that the longitudinal turbulent intensity decays with downstream distance following a power law. Figure 6 shows the decay of the longitudinal velocity fluctuation measured by hot-wire anemometry. The exponent of the decay law (≈ -0.79) is close to the one obtained by Blin[28] with a grid of similar dimension in a supersonic flow. At the opposite, Honkan and Andreopoulos[26] and Comte-Bellot and Corrsin[31,32] found values in the range of -1.2 for subsonic decaying turbulence. As expected, the longitudinal integral length scale

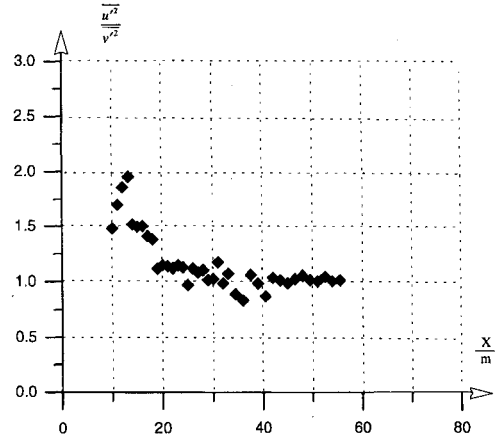

Fig. 4 Evolution of the anisotropy ratio along the wind-tunnel axis (the downstream distance X is here scaled on the multinozzle mesh size m).

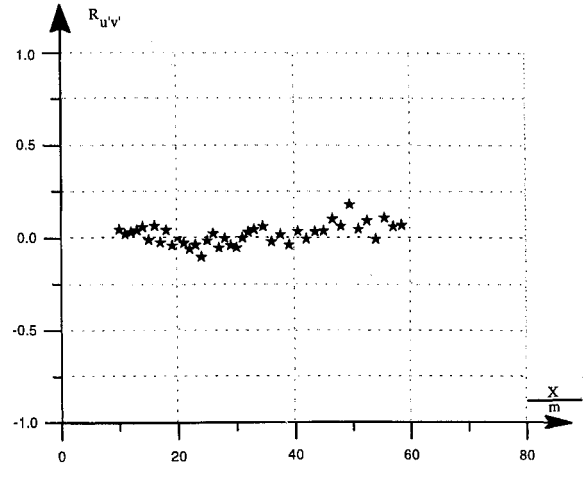

Fig. 5 Axial evolution of the longitudinal to lateral velocity fluctuations correlation coefficient (the downstream distance X is here scaled on the multinozzle mesh size m).

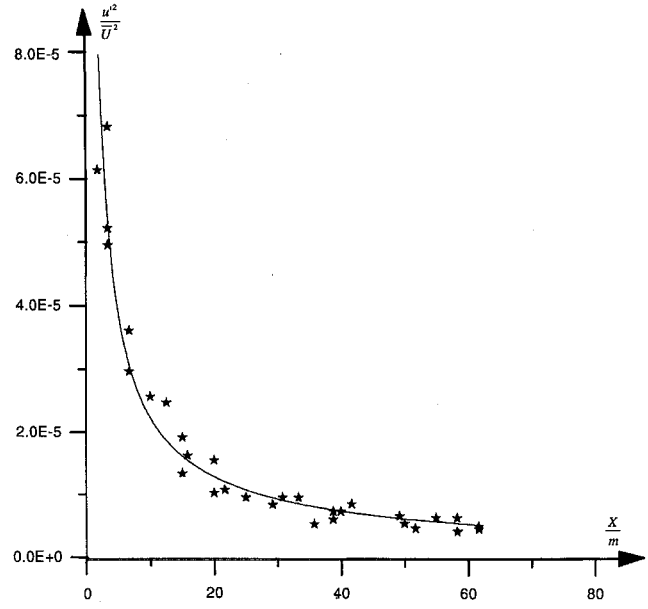

Fig. 6 Longitudinal decay of the velocity fluctuations along the wind-tunnel axis (the downstream distance X is here scaled on the multinozzle mesh size m); *, experimental result and ——, $(\overline{u'^2}/\overline{U^2}) = 1.37 \times 10^{-4} (X/M)^{-0.79}$.

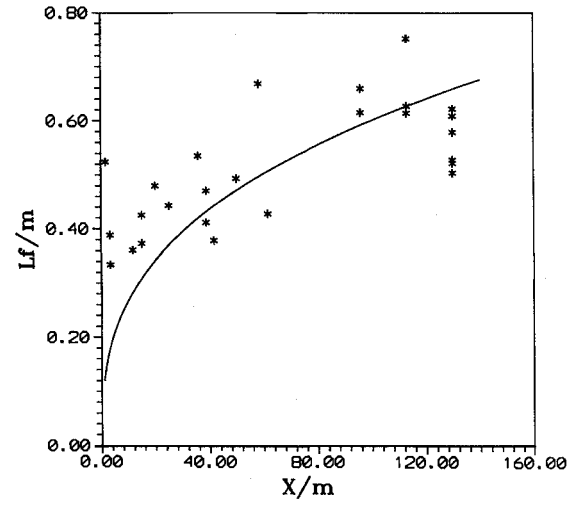

Fig. 7 Axial evolution of the longitudinal integral scale along the wind-tunnel axis (Lf and X are both related to the mesh size m).

was found to increase with downstream distance following a power law that is also comparable to subsonic grid flows cases[31,32] (see Fig. 7). It has to be noted that the measurement of the integral turbulent scale is a very difficult task in this Mach 3 turbulent flow. This can explain the relatively large scatter shown on Fig. 7. However, the law proposed by Comte-Bellot and Corrsin[31,32] seems to fit quite closely the present experimental data. It is difficult to compare the present results with those of Honkan and Andreopoulos[26] because their measurements deal with dissipation scales and not integral scales as in the present experiment.

B. Study of the Shock Wave/Turbulence Interaction

1. Mean Flow

The shock generator system is placed in the test section at a distance of $X = 460$ mm ($\approx$75 mesh size) downstream the multinozzle. Figure 8 shows a continuous (exposure time of 1 ms) schlieren photograph of the Mach effect. It can be observed that the two primary shock waves coming from the shock generators interact to create a Mach effect (i.e., normal shock wave) about 15 mm high in the center of the test section spanning in the entire wind tunnel. The shock surface is then $\approx 150 \times 15$ mm^2. Downstream, reflected shock waves and small mixing layers originated by the edges of the Mach effect

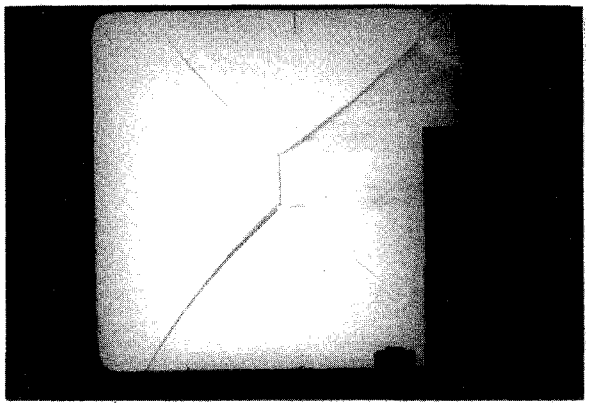

Fig. 8 Schlieren photograph (1-ms exposure time) of the Mach effect; X = 460 mm downstream of the multinozzle (flow is from left to right).

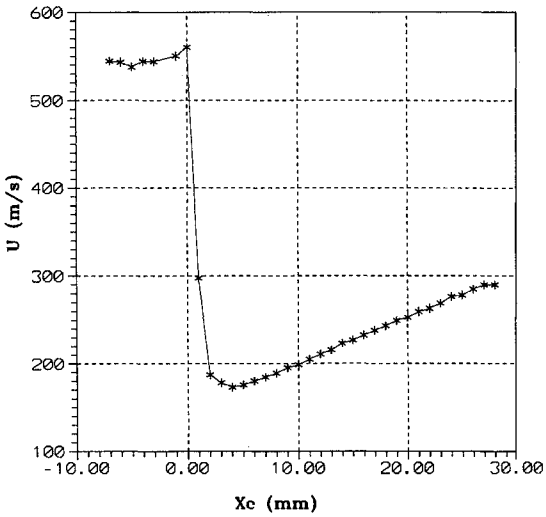

Fig. 9 Evolution of the mean longitudinal velocity across the interaction (Xc = 0 corresponds to the shock location).

are present. From this picture it appears that the images of the shock waves are very thin, typically less than 1 mm. We can then assume that the studied normal shock wave is unaffected by high-amplitude parasitic unsteadiness.

The interaction will be studied along the wind-tunnel axis in the center of the Mach effect to avoid shock curvature and boundary problems. At this location the incoming measured turbulence level is $\langle u' \rangle / U = 0.23\%$, giving a Mach number fluctuation of $\langle m' \rangle = 0.0061$, which is in the range of the values studied by Honkan and Andreopoulos[26] ($0.005 < \langle m' \rangle < 0.019$). The turbulent Reynolds number based on the mass flux fluctuations and on the mesh size is then $Rey = 5.83 \times 10^2$. The Reynolds number based on the mean mass flux and on the mesh size is $Rey_M = 5.5590 \times 10^4$. The evolution of the mean longitudinal velocity measured with a laser Doppler velocimeter (LDV) is shown in Fig. 9. It appears that the subsonic flow developing downstream of the normal shock is accelerated because of the growing of the Mach effect edges shear layers. The rapid distortion theory[33] has been applied to this flow to compute the effect of this acceleration on the turbulent field. Results show that these effects are negligible. It is interesting to notice that this LDV measurement is not able to provide the theoretical value of the velocity immediately downstream the shock (140 m/s in the present case). A transition zone about 3 mm thick where the measured velocity lies above the theoretical value is necessary to recover the correct evolution of the flow velocity. This effect is attributed to the inertia of the seeding particles used for laser Doppler measurements as stated, among others, by Leuchter et al.[34]

2. Turbulence Amplification in the Interaction

The longitudinal velocity fluctuations across the interaction are measured using the constant temperature hot-wire anemometer (CTA). The aim was to measure the ratio $\overline{u'^2}/\overline{u_0'^2}$ across the interaction ($\overline{u'^2}$ is the variance of the longitudinal velocity fluctuations and $\overline{u_0'^2}$ the initial level just before the shock).

It is well known that a CTA operated at a high enough overheat ratio (about 0.8 in the present experiment) is mainly sensitive to mass flux fluctuations.[35] To deduce the velocity fluctuations variance from a CTA measurement operated at a single overheat ratio, it is necessary to use classical assumptions like the so-called Morkovin hypothesis or strong Reynolds analogy (SRA).[36,37] This leads to the use of a velocity–temperature correlation coefficient of -0.9 that is a classical value in adiabatic supersonic flows.[38] Another problem concerning the use of hot wire is that, after the shock wave, the flow is mainly transonic (the Mach number varies from 0.5 to 1). It has been shown by Morkovin[39] that in this Mach number range and under some Reynolds number and overheating conditions the hot wire could be sensitive to Mach number fluctuations and then require a particular care for the calibration.[40] For the present measurements the hot wire is operated at an overheat ratio of 0.8 that is quite high. The Reynolds number based on stagnation conditions and on the wire diameter is about 10. From Horstmann and Rose's[41] calibration it appears that under these operating conditions the transonic effect on hot-wire calibration remains very low. The sensitivity coefficients given by Ardonceau[18] are used to process the experimental data because they were obtained in the same operating conditions, in the same wind tunnel with the same anemometer and with identical probes.

The turbulent field across the interaction was assumed to be isobaric. This means that pressure fluctuations are neglected when processing hot-wire data. The velocity fluctuations are then deduced from hot-wire measurements using the method described in Barre et al.[40] In the incoming turbulent flow, this assumption seems quite valid. We have noticed that small intensity Mach waves originating at the trailing edge of the multinozzle are strongly damped and have no influence on the homogeneity of the incoming flow at the location of the interaction. Furthermore, the incoming turbulence level is very low near the interaction (typically 1% rms mass flux fluctuations), giving a very low value for the fluctuating Mach number. Therefore, it is possible to assume that the incoming turbulent field is isobaric and incompressible. This assumption does not apply immediately downstream of the shock wave because of the sound generated by the shock/turbulence interaction.[5,6] It can be assumed that in this zone the turbulent field is formed from two fields. A first one is a pure acoustic field, and the second is an isobaric one where the SRA holds.[37] From Ribner's theory, for a Mach 3 normal shock wave, the pure acoustic field energy is predicted to represent about 40% of the total turbulent kinetic energy just after the shock. These acoustic waves are quickly damped and the asymptotic turbulent field remains isobaric. Blin[28] showed that, from Ribner's theory, it appears that, sufficiently downstream of the shock (Ribner's far field), the contribution of acoustic fluctuations to the turbulent energy is only about 2%.

Figure 10 shows the evolution of $\overline{u'^2}/\overline{u_0'^2}$ across the interaction. These values are deduced from hot-wire measurements using the isobaric turbulent field assumption.

Following the aforementioned discussion, data obtained in the immediate downstream vicinity of the shock are questionable. Note, however, that the complete resolution of this problem will require independent knowledge of the acoustic intensity just after the shock. This is a very difficult experimental task because of the very high pressure fluctuations frequency range expected in this area.

It can be seen from the present results that the measured longitudinal velocity fluctuations amplification is quite close to the one predicted by Ribner's theory. Concerning the near field, the value obtained, although neglecting acoustic waves intensity, gives an amplification ratio of the same order of magnitude of Ribner's theory predictions.

From hot-wire data it is also possible to have an idea of the distortion imposed on the incoming turbulence by the shock wave. Figure 11 shows the evolution of the skewness and flatness factor of the hot-wire signal fluctuations (which can be considered, in the present condition, as very close to the mass flux fluctuations) across the interaction.

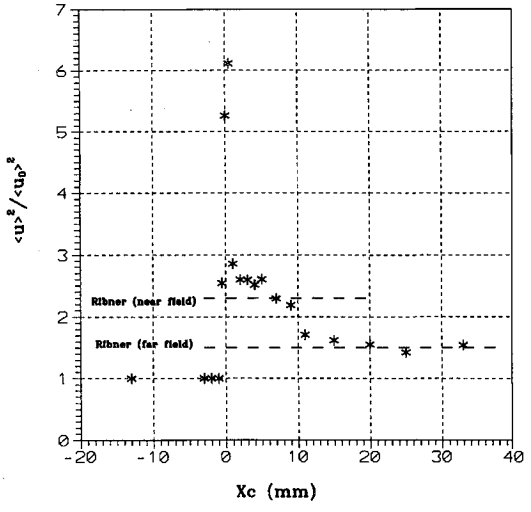

Fig. 10 Amplification of the longitudinal velocity fluctuations across the interaction.

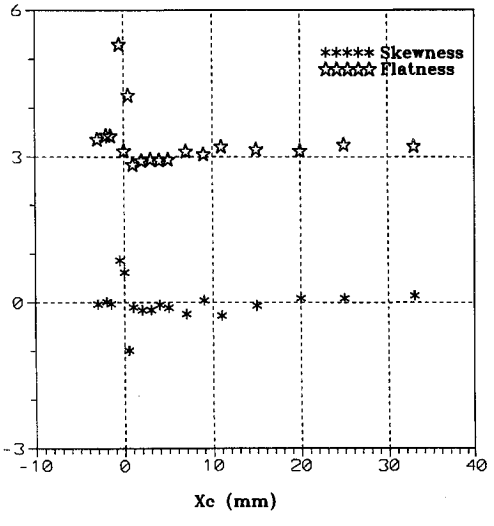

Fig. 11 Evolution of skewness and flatness factors of the hot-wire signal across the interaction.

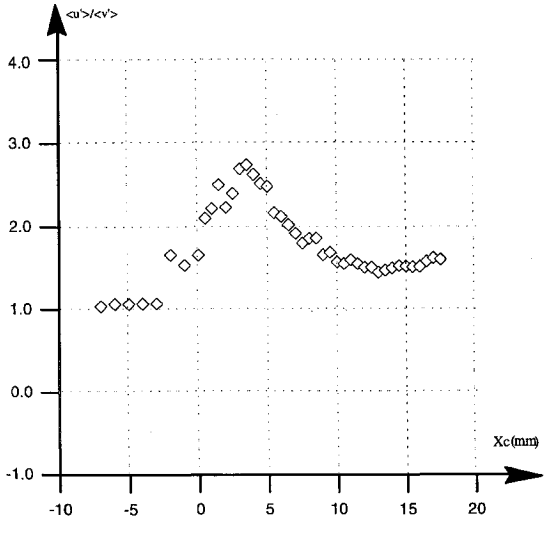

Fig. 12 Evolution of the anisotropy ratio $\langle u' \rangle / \langle v' \rangle$ across the shock wave (Xc = 0 corresponds to the shock location).

The incoming turbulence has quasi-Gaussian characteristics. This is also the case in the downstream field. In the near field, just after the shock, turbulence is strongly perturbed, but after a very short distance (about 2 mm) the field recovers its Gaussian structure. Figure 12 shows the evolution of the anisotropy parameter $\langle u' \rangle / \langle v' \rangle$ across the shock wave. It is clear that, after a strong distortion just after the shock wave, an asymptotic value of about 1.5 is finally obtained, confirming that the shocked turbulent field is now axisymmetric. The w' component has not been measured here, but because of the geometrical properties of the flow, it can be assumed that v' and w' components behave in the same way across the shock.

3. Turbulent Length Scale Evolution

From the hot-wire signal, it is possible to evaluate the longitudinal and lateral turbulent integral length scales.

For the longitudinal integral temporal scale, a simple integration of the autocorrelation function of the hot-wire signal is sufficient. We can transform this temporal value in a spatial scale using the Taylor hypothesis based on the measured local mean velocity. The evolution of the obtained integral length scale is plotted on Fig. 13 where the ratio Lf/Lf_0 is given across the interaction; Lf is the local integral length scale of each point and Lf_0 is the incoming value. An important decrease ($Lf/Lf_0 \approx 1/7$) is observed across the shock wave.

The lateral integral turbulent length scale can be measured using two hot wires placed at several distances along the Z axis. Figure 14

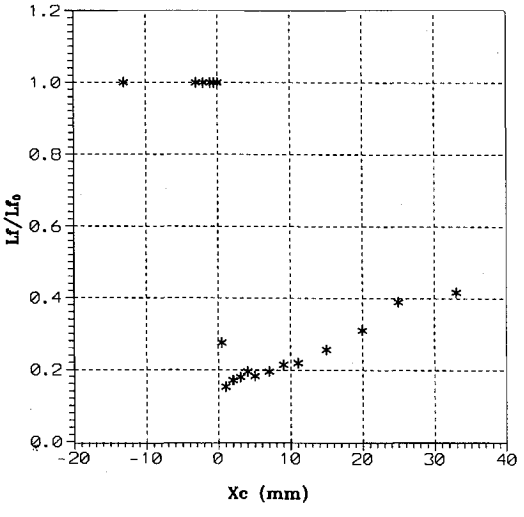

Fig. 13 Evolution of the longitudinal integral turbulent length scale across the interaction.

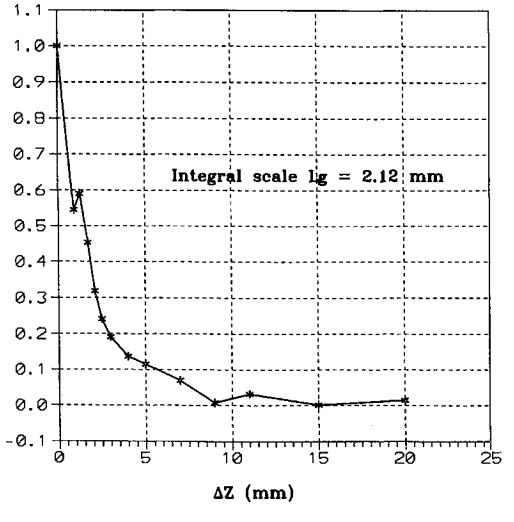

Fig. 14 Lateral correlation function just upstream the shock wave (X = 460 mm).

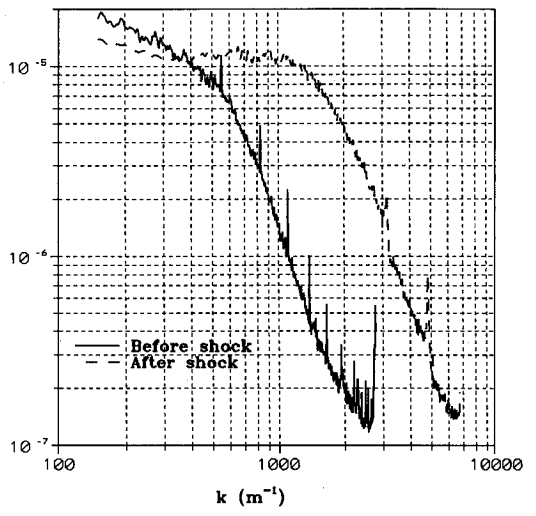

Fig. 15 Normalized hot-wire spectra just before and 11 mm (≈2 mesh grid size) downstream of the shock wave.

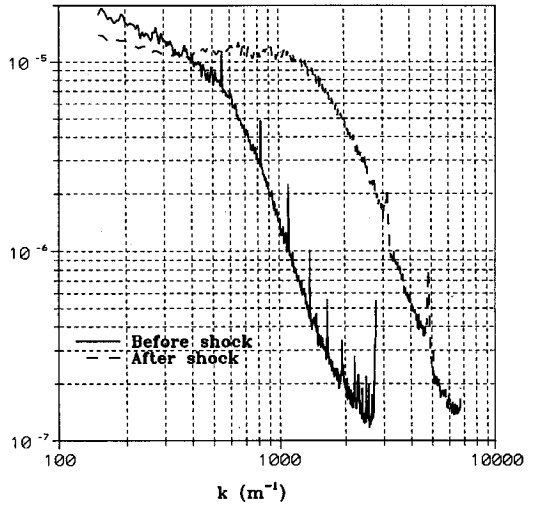

Fig. 16 Ratio of normalized hot-wire spectra just before and 11 mm (≈2 mesh grid size) downstream of the shock wave.

shows an example of such a lateral correlation function obtained for the incoming turbulence just before the shock location. The integration of this function gives the value of the lateral integral turbulent scale (Lg). In the present experiment a ratio $Lf/Lg \approx 2$ was found for the incoming turbulence. This value is quite similar to the one obtained in subsonic grid flows.[31,32] Some complementary measurements downstream of the shock wave showed that the lateral integral scale seems to be unaffected by the shock interaction.

Figure 15 shows two typical hot-wire signal spectra obtained before and after the shock. Wave numbers are calculated using the Taylor hypothesis with the local mean velocity. The two spectra presented in Fig. 15 are normalized by their own variances to be qualitatively comparable. It should be noticed that the nondimensionalization of the wave number is still an open problem, and we prefer here to provide dimensional wave numbers. It is obvious that higher wave numbers are present after the shock and that the amplification of the turbulence across the shock seems proportional to wave number. This interpretation can be confirmed by computing the ratio of the two spectra. The result is presented in Fig. 16. It appears then, in a wide range of wave numbers, that the amplification of the turbulent energy is proportional to wave number.

IV. Discussion

A fundamental shock wave/free turbulence interaction experiment is performed. A new method, based on a multinozzle concept, is developed to generate a clean turbulence in a Mach 3 supersonic flow. After qualification of the flow, the interaction of this turbulent field with a normal shock wave generated by a Mach effect is studied by means of hot-wire and laser Doppler velocimetry methods.

The turbulent field generated by this technique is quasihomogeneous and isotropic and can be considered free from strong acoustic effects if it is studied at a sufficiently long downstream distance (more than 10 mesh size) from the multinozzle. The evolution of the turbulent kinetic energy and of the turbulent length scales during the decay process of this turbulent field is similar to the one obtained in subsonic grid flows. We found, in particular, that the longitudinal to lateral integral scales ratio (Lf/Lg) is of the order of 2 as in subsonic grid flows.

Downstream of the shock interaction the longitudinal velocity fluctuations are amplified by a factor of about 2 in the near field and 1.5 in the far field. These values are in quite close agreement with the predictions of Ribner's linear theories. Longitudinal turbulent length scales are decreased by a factor close to 7 in the shock interaction. Consequently, turbulent spectra downstream of the shock exhibit more energy in the higher wave numbers range than in the incoming flow. The turbulent energy amplification, which is close to 1 for low wave numbers (up to 500 m^{-1}) increases to typically 25 for the higher measured wave number of the incoming turbulence (≈2000 m^{-1}). This result contradicts those of Refs. 24–27 in which the amplification of the kinetic energy is found to be more pronounced for low wave numbers. Complementary measurements have shown that the lateral integral scales are unaffected by the shock. It can then be concluded that the homogeneous and isotropic initial turbulent field becomes axisymmetric after the shock interaction.

Acknowledgments

The authors would like to acknowledge M. S. Sapin for the experiments. Many helpful conversations with L. Jacquin and J. F. Debiève are appreciated.

References

[1]Green, J. E., "Interactions Between Shock Waves and Turbulent Boundary Layers," *Progress in Aeronautical Sciences*, Vol. 11, 1970, pp. 235–340.

[2]Korkegi, R. H., "Comparison of Shock Induced Two- and Three-Dimensional Incident Turbulent Separation," *AIAA Journal*, Vol. 13, No. 4, 1974, pp. 534, 535.

[3]Fernholz, H. H., and Finley, P. J., "A Further Compilation of Compressible Boundary Layer Data with a Survey of Turbulence Data," AGARDograph No. 263, 1981.

[4]Ribner, H. S., "Convection of a Pattern of Vorticity Through a Shock Wave," NACA TN-2864, 1953.

[5]Ribner, H. S., "Shock-Turbulence Interaction and the Generation of Noise," NACA TN-3255, 1954.

[6]Ribner, H. S., "Acoustic Energy Flux from Shock-Turbulence Interaction," *Journal of Fluid Mechanics*, Vol. 35, 1969, pp. 299–310.

[7]Moore, F. K., "Unsteady Oblique Interaction of a Shock Wave with a Plane Disturbance," NACA TN-2879, 1953.

[8]Kerrebrock, J. L., "The Interaction of Flows Discontinuities with Small Disturbances in a Compressible Fluid," Ph.D. Thesis, California Inst. of Technology, Pasadena, CA, 1956.

[9]Chang, C. T., "Interaction of a Plane Shock and Oblique Plane Disturbances with Special Reference to Entropy Waves," *Journal of the Aeronautical Sciences*, Vol. 24, 1957, pp. 675–682.

[10]McKenzie, J. F., and Westphal, K. O., "Interaction of Linear Waves with Oblique Shock Waves," *Physics of Fluids*, Vol. 11, 1968, pp. 2350–2362.

[11]Kovasznay, L. S. G., "Turbulence in Supersonic Flow," *Journal of the Aeronautical Sciences*, Vol. 20, 1953, pp. 657–682.

[12]Rotman, D., "Shock Wave Effect on a Turbulent Flow," *Physics of Fluids A*, Vol. 3, No. 7, 1991, pp. 1792–1806.

[13]Lee, S., Lele, S. K., and Moin, P., "Direct Numerical Simulation of Isotropic Turbulence Interacting with a Weak Shock Wave," *Journal of Fluid Mechanics*, Vol. 251, 1993, pp. 533–562 (Corrigendum, Vol. 264, 1994, pp. 373, 374).

[14]Lee, S., Lele, S. K., and Moin, P., "Interaction of Isotropic Turbulence with a Strong Shock Wave," AIAA Paper 94-0311, 1994.

[15]Hannappel, R., and Friedrich, R., "Interaction of Isotropic Turbulence with a Normal Shock Wave," 4th European Turbulence Conf., Delft, The Netherlands, July 1992.

[16]Smits, A. J., and Muck, K. C., "Experimental Study of Three Shock Wave/Boundary Layer Interactions," *Journal of Fluid Mechanics*, Vol. 182, 1987, pp. 294–314.

[17]Andreopoulos, J., and Muck, K. C., "Some New Aspect of the Shock Wave Boundary Layer Interaction in Compression Ramp Corner," *Journal of Fluid Mechanics*, Vol. 180, 1987, pp. 405–428.

[18]Ardonceau, P., "The Structure of Turbulence in a Supersonic Shock Wave/Boundary Layer Interaction," *AIAA Journal*, Vol. 22, No. 9, 1984, pp. 1254–1262.

[19]Dolling, D. S., and Murphy, M., "Wall Pressure in a Supersonic Separated Compression Ramp Flowfield," AIAA Paper 82-0986, 1982.

[20]Settles, G. S., Williams, D. R., Baca, B. K., and Bogdonoff, S. M., "Reattachment of a Compressible Turbulent Free Shear Layer," *AIAA Journal*, Vol. 20, No. 1, 1982, pp. 60–67.

[21]Hayakawa, K., Smits, A. J., and Bogdonoff, S. M., "Turbulence Measurements in a Compressible Reattaching Shear Layer," *AIAA Journal*, Vol. 22, No. 7, 1984, pp. 889–895.

[22]Samimy, M., and Addy, L., "A Study of Compressible Turbulent Reattaching Free Shear Layers," AIAA Paper 85-1646, 1985.

[23]Jacquin, L., Blin, E., and Geffroy, G., "Experiments on Free Turbulence/Shock Wave Interactions," 8th Symposium on Turbulent Shear Flows, Munich, Germany, 1991.

[24]Troiler, J. W., and Duffy, R. E., "Turbulent Measurements in Shock Induced Flows," *AIAA Journal*, Vol. 23, No. 8, 1985, pp. 1172–1178.

[25]Hartung, L. C., and Duffy, R. E., "Effects of Pressure on Turbulence in Shock-Induced Flows," AIAA Paper 86-0127, 1986.

[26]Honkan, A., and Andreopoulos, J., "Rapid Compression of Grid Generated Turbulence by a Moving Shock Wave," *Physics of Fluids A*, Vol. 4, No. 11, 1992, pp. 2562–2572.

[27]Keller, J., and Merzkirch, W., "Interaction of a Normal Shock Wave with a Compressible Turbulent Flow," *Experiments in Fluids*, Vol. 8, 1990, pp. 241–248.

[28]Blin, E., "Etude expérimentale de l'interaction entre une turbulence libre et une onde de choc," Thèse de doctorat de l'Université Paris VI, Paris, France, 1993.

[29]Debiève, J. F., and Lacharme, J. P., "A Shock Wave/Free Turbulence Interaction," *Turbulent Shear Layer/Shock Wave Interactions*, edited by J. Délery, Springer–Verlag, Berlin, 1986.

[30]Bonnet, J. P., and Alziary, T., "Determination and Optimization of Frequency Response of Constant Temperature Hot-Wire Anemometers in Supersonic Flows," *Review of Scientific Instruments*, Vol. 51, Feb. 1980, pp. 234–239.

[31]Comte-Bellot, G., and Corrsin, S., "The Use of a Contraction to Improve the Isotropy of Grid-Generated Turbulence," *Journal of Fluid Mechanics*, Vol. 25, 1966, pp. 657–682.

[32]Comte-Bellot, G., and Corrsin, S., "Simple Eulerian Time Correlation of Full and Narrow-Band Velocity Signals in Grid-Generated, 'Isotropic' Turbulence," *Journal of Fluid Mechanics*, Vol. 48, Pt. 2, 1971, pp. 273–337.

[33]Jacquin, L., Cambon, C., and Blin, E., "Turbulence Amplification by a Shock Wave and Rapid Distorsion Theory," *Physics of Fluids A*, Vol. 5, No. 10, 1993, pp. 2539–2550.

[34]Leuchter, O., Amram, K., and Thomas, P., "Etude théorique et expérimentale du comportement des particules à la traversée d'une onde de choc," 3ème Congrès francophone de vélocimétrie Laser, Toulouse, France, Sept. 1992.

[35]Smits, A. J., and Dussauge, J. P., "Hot Wire Anemometry in Supersonic Flow," AGARDograph No. 315, 1989.

[36]Gaviglio, J., "Sur les méthodes de l'anémométrie par fil chaud des écoulements compressibles des gaz," *Journal de Mécanique Appliquée*, Vol. 2, No. 4, 1978, pp. 449–498.

[37]Gaviglio, J., "Reynolds Analogies and Experimental Study of Heat Transfer in the Supersonic Boundary Layer," *International Journal of Heat and Mass Transfer*, Vol. 30, No. 5, 1987, pp. 911–926.

[38]Dupont, P., and Debiève, J. F., "A Measurement Method of Temperature and Velocity Fluctuations from Transonic to Supersonic Regimes," European Telemetry and Test Conf., Marseille, France, June 1989.

[39]Morkovin, M. V., "Fluctuations and Hot Wire Anemometry in Compressible Flow," AGARDograph No. 24, 1956.

[40]Barre, S., Dupont, P., and Dussauge, J. P., "Hot Wire Measurements in Turbulent Transonic Flows," *European Journal of Mechanics, B/Fluids*, Vol. 11, No. 4, 1992, pp. 439–454.

[41]Horstman, C. C., and Rose, W. C., "Hot Wire Anemometry in Transonic Flows," *AIAA Journal*, Vol. 15, No. 3, 1977, pp. 395–401.